

Galvanic Coupling between Carbon Steel and Stainless Steel Reinforcements

Shiyuan Qian

Institute for Research in Construction

National Research Council Canada, Ottawa, Canada, K1A 0R6

Deyu Qu

Physical Chemistry Laboratory, Division of Chemistry, Graduate School of Science,

Hokkaido University, Sapporo, Japan

Gary Coates

Nickel Institute

55 University Ave, Suite 1801

Toronto, ON, Canada M5J 2H7

ABSTRACT

Galvanic corrosion is a potentially major concern associated with the application of stainless steel reinforcement which is in direct (electrical) contact with carbon steel reinforcement in concrete structures. Judicious use of stainless steel rebar in both new construction and rehabilitation of older structures is a viable, cost-effective option for extending service life and reducing maintenance costs. Questions, however, had arisen about the possibility of increased corrosion due to galvanic effects. This paper investigates the galvanic-coupling behaviours of three different types of stainless steel and carbon steel. Tests were performed both in electrochemical cells and with specimens in concrete inside an environmental chamber. The results show that oxygen reduction on stainless steel is the rate-determining factor for galvanic coupling of these two metals. It is much lower than that of passive carbon steel. As a result, the galvanic coupling of stainless steel with carbon steel will not increase the risk of corrosion of carbon steel reinforcement.

Keywords: galvanic coupling; stainless steel; reinforcement corrosion; chloride; cyclic voltammograms.

CANADIAN INST. OF MINING, METALLURGY & PETROLEUM
44th ANNUAL CONF. OF METALLURGISTS
CALGARY, ALBERTA, CANADA
21-24 AUG. 2005

INTRODUCTION

Chloride-induced corrosion is the main cause of deterioration of conventional carbon-steel-reinforced concrete structures. Stainless steel, with its superior corrosion resistance, has been used to minimize the problems of reinforcement corrosion in many structures in the last 15 years. However, the use of this reinforcement is still limited, partially because of its higher initial cost. Therefore, a potentially economical approach is to use stainless steel in areas of the structure where corrosion is most likely to occur because the reinforcement will be surrounded by the most aggressive environment. This will significantly extend the service life of concrete structures with only a slight increase in the initial cost and will deliver reduced life cycle costs. This approach can also be used in the rehabilitation of deteriorated reinforced-concrete structures. While there has been considerable interest in this approach, there have been concerns about galvanic corrosion, as these dissimilar metals will most often be in direct (electrical) contact in concrete structures. Most engineers are aware that there is a potential risk for galvanic corrosion between the more noble stainless steel and the less noble carbon steel. As a result, they are often hesitant to use stainless steel and carbon steel in the same concrete structure. However, many engineers are not aware that there is also a potential galvanic effect between carbon steel that is in the active (corroding) state with carbon steel in the passive (non-corroding) state. This galvanic effect can occur within the same rebar.

Limited investigations have been published, but the results and conclusions are controversial. Bertolini et al. (1-3) concluded from their experiments on concrete specimens that the use of stainless steel in combination with carbon steel did not increase the risk of corrosion of passive carbon steel. Galvanic coupling with stainless steel can increase the corrosion rate of active carbon steel reinforcement in chloride-contaminated concrete, but the effect is no worse than in the coupling with passive carbon steel. Knudsen et al. (4, 5) and Klinghoffer et al. (6) suggested that the use of carbon steel with stainless steel does not increase the risk of corrosion for the carbon steel, as long as both metals are in a passive condition. Cochrane (7) reached a similar conclusion. Hope concluded in his study (8) that high and potentially damaging corrosion rates would develop in galvanically coupled carbon steel and stainless steels 316 or 2205 if the concrete surrounding the carbon steel becomes chloride-contaminated or carbonated. These corrosion rates are likely to be similar to, or somewhat less than, the corrosion rates if carbon steel alone were used.

However, Webster (9) addressed this problem and determined that corrosion could take place if two different metals were electrically connected. He also suggested that it would be necessary to isolate the electron transfer path between the anode and the cathode to prevent corrosion damage due to galvanic coupling. Seibert (10) stated that coupling carbon steel with stainless steel reinforcements is not recommended because this galvanic coupling would initiate corrosion on the carbon steel.

This paper presents an investigation of the galvanic coupling behaviour between carbon steel (CS) and three types of stainless steel (SS) alloys. Tests were performed both in electrochemical cells containing saturated calcium hydroxide solution $[\text{Ca}(\text{OH})_2]$ and with concrete specimens inside a environmental chamber. Sodium chloride (NaCl) was introduced to the solution during the experiment or premixed in the concrete, to simulate aggressive environmental conditions from road salt in the field. The galvanic coupling currents between corroding CS and SS were measured and compared with those between corroding CS and passive CS, which always surrounds the corroding area. The anodic/cathodic behaviours of individual CS and SS were also studied using the potential polarization test, and cyclic voltammetry. The effects of the oxygen reduction rate, coupling resistance and chloride content on the galvanic coupling current were also investigated.

EXPERIMENTAL

Electrodes and Solutions

The electrodes were machined from reinforcing CS and SS bars (2205, 304LN and 316LN – see Table 1 for nominal compositions) to two sizes: a small sample (15 mm in length and 9.5 mm in diameter) and a large sample (70 mm in length and 12.5 mm in diameter). The samples were screwed to a CS or SS rod, respectively, as the electric conductor. The steel rod was isolated from the solution by a glass tube. The samples were then embedded in epoxy resin leaving a fixed steel surface exposed to the solution. The surface areas of the small and large electrodes were 0.7 cm^2 and 28.6 cm^2 , respectively. The samples were polished with #600 silicon-carbide papers and then immersed in saturated calcium hydroxide $[\text{Ca}(\text{OH})_2]$ solution with a pH of 12.6 for a week. The corroding CS samples were prepared by placing them in a humidity room to let the rust accumulate on their surfaces. The electrochemical experiments were carried out in a saturated $\text{Ca}(\text{OH})_2$ solution or a saturated $\text{Ca}(\text{OH})_2 + 3\% \text{ NaCl}$ solution. De-ionized water ($\geq 18.3 \text{ M}\Omega \text{ cm}^2$, Milli-Q) was used to prepare the solution and high-purity argon and oxygen were used in some experiments to respectively purge or dissolve oxygen in the solution.

Table 1 - Nominal Chemical Composition of Tested Stainless Steel Alloys (wt %).

Alloy	C (max)	Cr	Ni	Mo	N
304LN	0.03	19	9	-	0.12
316LN	0.030	17	11	2.2	0.12
2205	0.030	22	5.5	3.0	0.15

Concrete Specimens

Galvanic coupling tests were carried out on different pairs of rebars in concrete specimens. The compositions of the concrete mixtures and the compressive strength of the cylindrical specimens are listed in Table 2. The specimens were cured for 35 days in a $95\% \pm 5\%$ relative humidity (RH) and $22 \pm 2^\circ\text{C}$ environment. Two rebars were embedded in parallel in concrete specimens. Different amounts of NaCl (weight of cement as shown in Table 2) were added to the concrete mixtures. The different combinations in the specimens are listed in Table 3. Three specimens were made for each combination. In each specimen, two ends of the rebar were coated with epoxy resin and covered by a shrinkable sleeve leaving a length of 15 cm (surface area $\approx 70.7 \text{ cm}^2$) exposed to the concrete.

Table 2 - Composition of Concrete Specimens (kg) for the Galvanic Coupling Tests.

NaCl	Cl ⁻ % (wt of cement)	Water	Cement	Fine aggregate	Coarse aggregate	7 days strength (MPa)
0	0	5.75	11.5	23	34.5	39.2
0.398	1.5	8.00	16.0	32	48.0	39.7
1.289	3.5	11.25	22.5	45	67.5	35.8

Table 3 - Rebar Specimens and Chloride Concentrations in Concrete.

Left side of specimens		Right side of specimens	
Chloride content (%)	Metal	Chloride content (%)	Metal
0	CS	0	SS*
0	CS	3.5	SS*
0	CS	0	CS
1.5	CS	0	SS*
1.5	CS	3.5	SS*
1.5	CS	0	CS

Note: * Includes SS 2205, 304LN and 316LN.

Measurements

The following electrochemical techniques were used in this study: cyclic voltammetry, linear polarization, potential dynamic and galvanic coupling measurements. All tests (except the galvanic coupling experiment) were conducted in three-compartment electrochemical cells. The working electrode was the CS or SS sample. The counter electrode was made of platinum foil or mesh. The reference electrode was a saturated calomel electrode (SCE). In this paper, all the potentials presented are relative to the SCE. A Luggin capillary was used to reduce the potential drop (iR drop) between the reference and working electrodes. The cyclic voltammetry, linear polarization and potential dynamic measurements were carried out using a

Solartron 1480 multistat or a Solartron SI 1287 electrochemical interface, which was controlled by a PC using *Corr-Ware* software.

Cyclic voltammograms were scanned at a rate of 20 mV/s; potential dynamic tests were measured at a rate of 0.1 mV/s. The linear polarization was measured at ± 10 mV around E_{corr} at a slow rate of 0.01 mV/s. The galvanic coupling experiments were carried out using a setup of two electrochemical cells connected by a salt bridge as shown in Figure 1. The galvanic current was measured and recorded by connecting the two metals using a Keithley 485 picoammeter controlled by a PC using *VEE pro* software. The salt bridge was made of a U-shaped glass tube with an internal diameter of either 9.4 mm or 3.1 mm. The two ends of the U-shaped glass tube were sealed with a Celgard[®] 2500 microporous membrane to prevent solution flow and reduce the chloride ion diffusion. The glass tube was filled with saturated $\text{Ca}(\text{OH})_2$ solution with or without 3% NaCl, depending on the experimental conditions. For the galvanic coupling experiment, corroding CS was always in the saturated $\text{Ca}(\text{OH})_2 + 3\%$ NaCl solution. The negative (black) terminal of the picoammeter was connected to the corroding CS when it was coupled with passive CS or SS, or connected to the passive CS when it was coupled with SS.

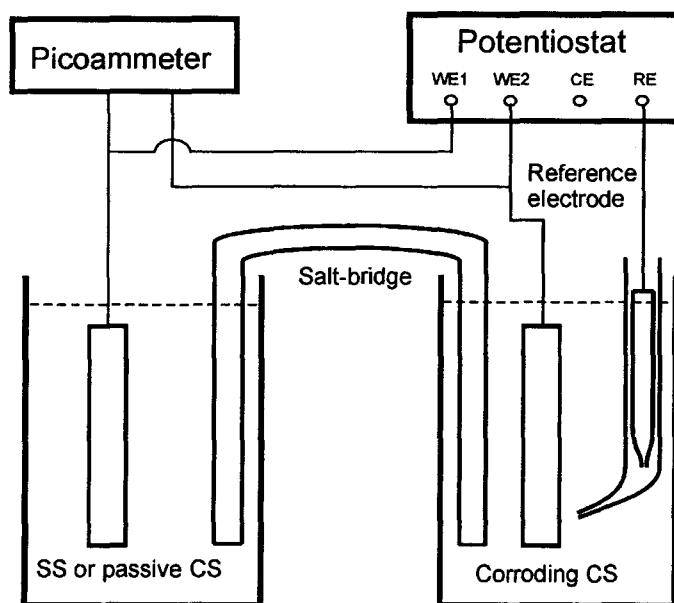


Figure 1 – Galvanic coupling measurement set-up.

Measurement of the galvanic coupling behaviour was also carried out on the steel rebars embedded in concrete specimens. Two parallel rebars were embedded in each concrete specimen, as shown in Figure 2. The two ends of the rebar were coated with epoxy resin and covered by a shrinkable sleeve, leaving a length of 15 cm (surface area = 70.7cm^2) exposed to the concrete. The concrete specimens were located in an

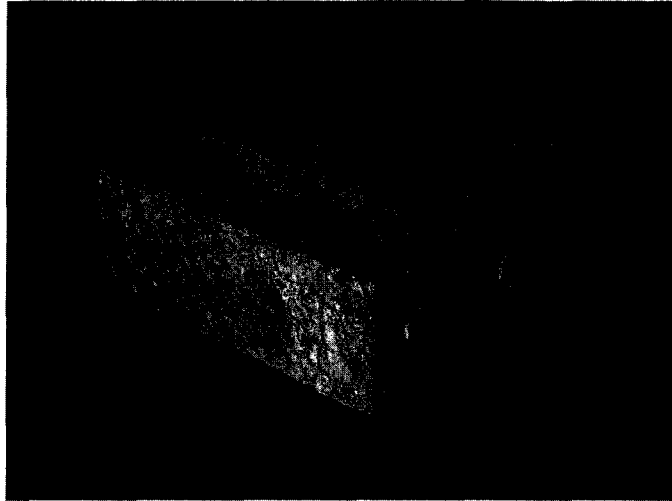


Figure 2. - Photo of a concrete specimen used in galvanic coupling tests

environmental chamber, in which the RH was kept at 80% and the temperature cycled between 25°C and 45°C each day to accelerate the corrosion process of the rebars. The upper temperature was changed from 45°C to 50°C during the stages corresponding to day 220 and 300 to further accelerate the corrosion process. The two rebars in each concrete specimen were connected by an external wire. The galvanic coupling current between these two rebars was measured using a Keithley 485 picoammeter. The coupling potential was measured using a Keithley 617 multimeter and a copper/copper sulphate (Cu/CuSO₄) reference electrode (converted relative to SCE). Both measurements were carried out on a weekly basis, and an average of three samples was plotted.

RESULTS AND DISCUSSION

Galvanic Coupling Current Density

Galvanic corrosion occurs when two (or more) dissimilar metals are electrically connected and exposed to an electrolyte (electrically conductive solution). The potentials of the two metals, after connection, are forced to shift to a common potential (or galvanic coupling potential, E_{gc}). The metal with an initially more negative potential (corroding CS) is subjected to an increased oxidation (anodic) process, since it is polarized toward the positive direction. The more noble metal (SS) with an initially more positive potential is polarized to the negative direction and subjected to an increased reduction (cathodic) process. The electrons transfer from the active metal to the noble one. The galvanic coupling current density, I_{gc} , shifts towards a stable value after an initial large current spike to charge the double layer of the electrode. This stable current is the measured I_{gc} , which is almost the cathodic current density on coupled SS.

The galvanic coupling current densities, I_{gc} , were measured by connecting corroding CS with passive CS or SS (2205, 304LN and 316LN) as shown in Figure 3. The currents gradually approached a stable value after the initial pulse. It is clearly shown that the galvanic coupling current between the corroding CS and SS is less than half of that between the corroding CS and the passive CS.

The corrosion rate of the corroding CS was measured using a linear polarization technique. The average rate (as measured by current density) was $13.3 \pm 0.4 \mu\text{A}/\text{cm}^2$ at a corrosion potential of -0.6 V vs SCE . The percentage increases in I_{gc} between the corroding CS and the passive CS or SS over the corrosion current density of the corroding CS are listed in Table 4. It is known that I_{gc} does not fully contribute to an increase in the corrosion of the corroding CS. It compensates partially (about 40% of I_{gc}) for the decrease in the cathodic current density and contributes partially (about 60%) to the increase in the corrosion current density, ΔI_{corr} , on the corroding CS. These values are calculated based on the experimental results showing that the Tafel slopes of anodic and cathodic polarization for corroding CS are 40 mV and 60 mV, respectively. Therefore, the increase in the corrosion rate is about 2.4% due to the galvanic coupling between the corroding CS and passive CS, and it is only 1.0% due to the galvanic coupling between the corroding CS and SS. It is clearly shown that the galvanic coupling effect introduced by SS is smaller than with passive CS and may be considered insignificant. The micro corrosion on the corroding CS itself is a dominant process in the corrosion of CS.

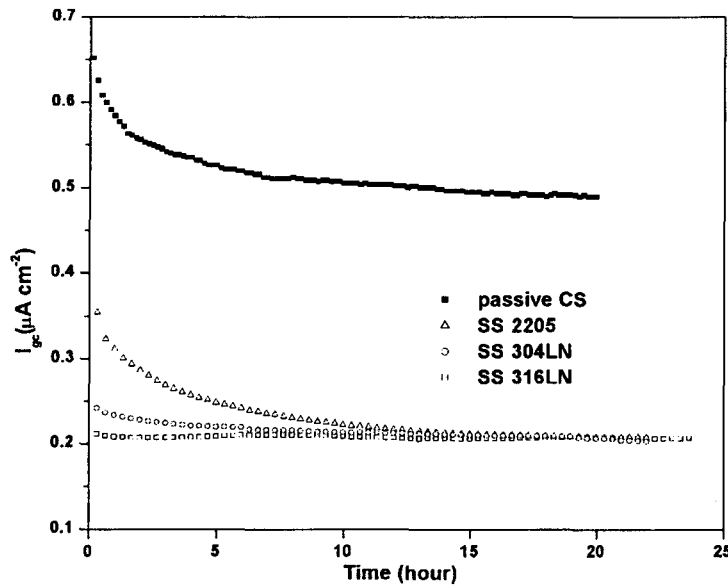


Figure 3 - I_{gc} measured by coupling corroding CS with passive CS or SS alloys in a saturated $\text{Ca}(\text{OH})_2$ solution.

Table 4 - Relationship between I_{gc} and I_{corr} for Various Metals Coupled to Corroding CS at -0.6 V vs. SCE.

Metals	I_{gc}/I_{corr} (%)	$\Delta I_{corr}/I_{corr}$ (%)
Passive CS	4.0	2.4
SS 2205	1.7	1.0
SS 304LN	1.7	1.0
SS 316LN	1.8	1.1

Note: I_{gc} is the average measured value.

Effect of Oxygen on Cathodic-Reduction Current

The cyclic voltammograms of passive CS and SS 2205, 304LN and 316 LN were measured in the saturated $\text{Ca}(\text{OH})_2$ solution as shown in Figure 4. The cathodic and anodic current densities of all SS alloys are significantly smaller than those of the passive CS. The corrosion potential of the corroding CS is about -0.55 V to -0.6 V. Therefore, the potential of galvanic coupling of corroding CS with passive CS or SS should be in this potential range, and the reactions on passive CS or SS are cathodic. From the inset of Figure 4, it can be clearly seen that the cathodic reduction current densities of all SS alloys are much smaller than those of the passive CS (solid line) in this potential range. Obviously, the surface of SS does not favour the process of cathodic reduction.

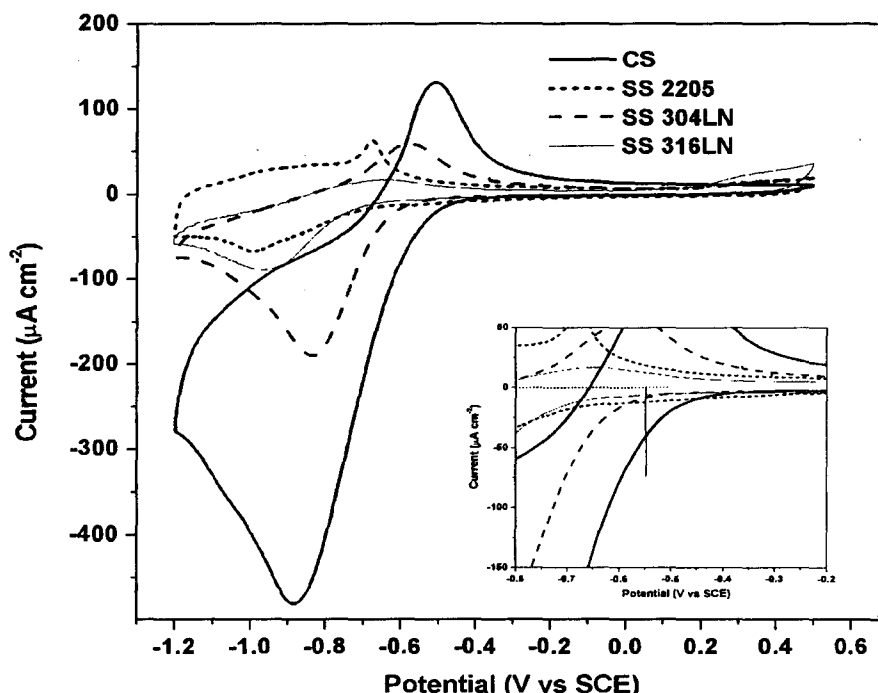


Figure 4 - Cyclic voltammograms of passive CS and SS measured in a saturated $\text{Ca}(\text{OH})_2$ solution (the inset shows an enlarged current scale).

The effect of dissolved oxygen on the cathodic reduction current density was investigated. First, a cyclic voltammogram of passive CS was measured in the cell open to the air. Oxygen was then bubbled into the cell to saturate the electrolyte solution, and another cyclic voltammogram was measured. After that, the solution in the cell was degassed by bubbling argon into the cell to remove the dissolved oxygen. The cyclic voltammogram was measured again. The cyclic voltammograms measured under these three conditions are shown in Figure 5. The cathodic current had the smallest peak with a value of $-180 \mu\text{A}/\text{cm}^2$ at -0.72 V when oxygen was purged from the solution. The charges for the cathodic and anodic scans are almost equal indicating that both reactions are mainly for the electrode surface oxidation and reduction. When the concentration of oxygen in the solution was increased (cell open to the air), the cathodic current peak increased to $-330 \mu\text{A}/\text{cm}^2$ at -0.87 V . When the electrolyte solution was saturated with oxygen, the cathodic current peak increased to the largest value of $-400 \mu\text{A}/\text{cm}^2$ at -1.0 V indicating that a significant oxygen reduction reaction was involved.

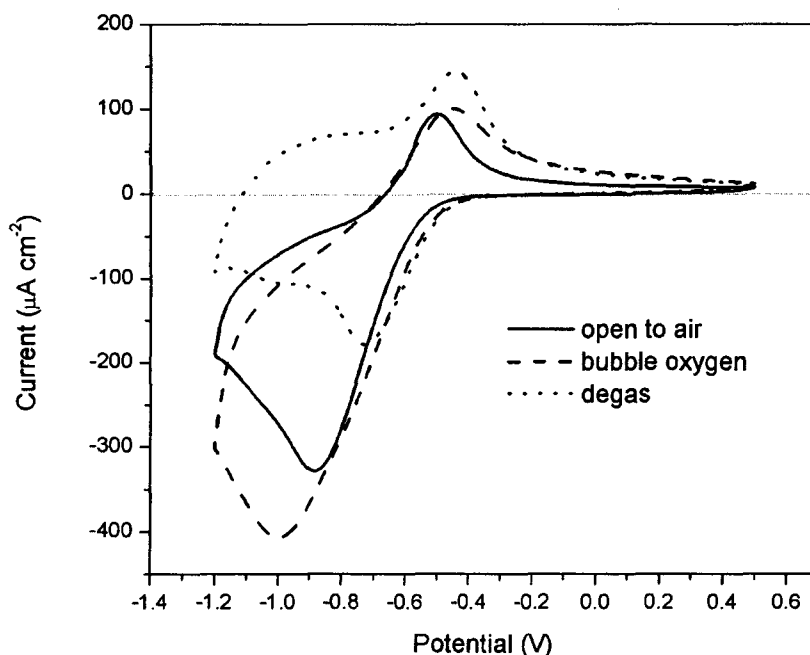


Figure 5 - Cyclic voltammograms of passive CS under various oxygen conditions.

In the potential region between -0.4 V and -0.72 V , the effect of oxygen concentration on the cathodic reaction was not observed, because the reduction of the oxidized metal surface dominated the reaction. The slight increase in the reduction currents under the conditions of bubbling oxygen and argon is probably caused by the increase in the diffusion process due to gas bubbling through the solution. In the anodic scan (from -1.2 V to -0.4 V), the current shifts to more negative values when open to air and bubbling oxygen, because of the process of continuing oxygen reduction. The

current increase in the more positive region (-0.4 V to +0.5 V) is due to the bubbling effect causing the increase in the diffusion process.

Figure 6 shows the cathodic polarization curves of the passive CS and the SS. The cathodic current densities on the three SS alloys are all much smaller than those in the passive CS in the range of -0.5 V to -0.6 V. As described above, I_{gc} is limited by the cathodic reduction reaction on the passive CS or SS when the corroding CS is coupled with them. Therefore I_{gc} induced by SS is much smaller than that induced by the passive CS when these metals are coupled with corroding CS.

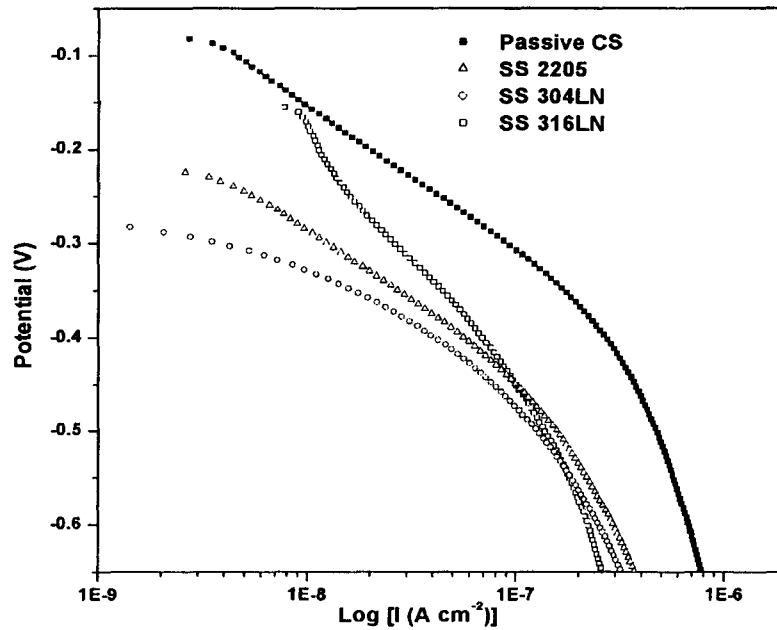


Figure 6 - Cathodic polarization curves of passive CS and SS measured in a saturated $\text{Ca}(\text{OH})_2$ solution.

Effect of Resistance of the Salt Bridge

Table 5 shows the change in the values of I_{gc} with the electrical resistance of the salt bridge measured by galvanic coupling experiments in an electrochemical cell. When the resistance of the salt bridge increases from 0.9 k Ω to 33.0 k Ω , I_{gc} decreases from 0.44 $\mu\text{A}/\text{cm}^2$ to 0.18 $\mu\text{A}/\text{cm}^2$ for the coupling between passive and corroding CS, and from 0.20 $\mu\text{A}/\text{cm}^2$ to 0.05 $\mu\text{A}/\text{cm}^2$ for the coupling between SS 316LN and corroding CS, respectively. It is clearly shown that I_{gc} decreases with increasing resistance of the salt bridge. It is important to notice that I_{gc} induced by SS 316LN is always much smaller than that induced by the passive CS regardless of the resistance change in the salt bridge. The effect of resistance in the salt bridge on the galvanic coupling is equivalent to the effect of resistance in concrete. The resistance changes from 0.9 k Ω to 33.0 k Ω cover a wide change in the concrete resistivity and corresponds to a wide range in the rebar

corrosion rates (from low to high) (11). Therefore, changes in I_{gc} with an increase in the resistance of the salt bridge have practical significance for simulating resistivity changes in concrete. With an increase in concrete resistance, the I_{gc} will decrease significantly.

Table 5 – Variations of Galvanic Coupling Current Density, I_{gc} with Resistances of Salt Bridge.

Resistance of salt bridge (k Ω)	0.9	2.3	33.0
I_{gc} ($\mu\text{A}/\text{cm}^2$) passive CS coupled with corroding CS	0.44	0.32	0.18
I_{gc} ($\mu\text{A}/\text{cm}^2$) SS 316LN coupled with corroding CS	0.20	0.18	0.05

Effect of Chloride Ions

Since SS has a much higher threshold of resistance to chloride-corrosion, it can be substituted for CS in critical areas with high concentration of chloride ions in order to extend the service life of concrete structures. The effect of SS surrounded by chloride ions on the galvanic coupling current is another important factor to evaluate in determining whether coupling CS with SS is a safe approach in such environments.

The galvanic-coupling current was investigated by coupling corroding CS with SS in a saturated $\text{Ca}(\text{OH})_2$ solution containing 3% NaCl, as shown in Figure 7 (inset).

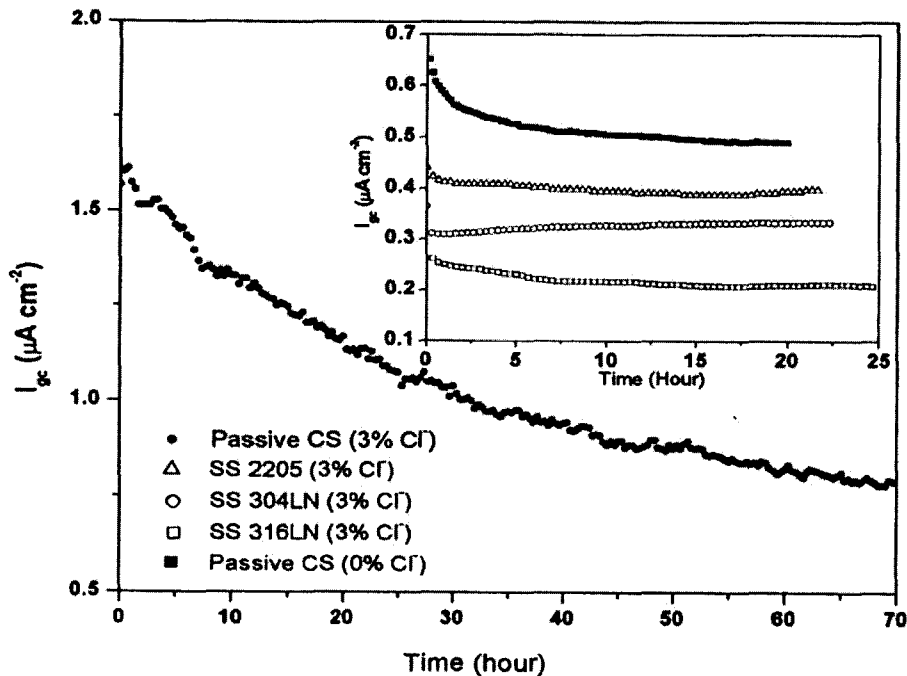


Figure 7 - I_{gc} measured by coupling corroding CS with passive CS or SS alloys in a saturated $\text{Ca}(\text{OH})_2$ solution containing 0% or 3% NaCl.

The average values of I_{gc} are $0.42 \mu\text{A}/\text{cm}^2$, $0.33 \mu\text{A}/\text{cm}^2$ and $0.23 \mu\text{A}/\text{cm}^2$ for SS 2205, 304LN and 316LN, respectively (see also Table 6). The curve of I_{gc} for passive CS coupled with corroding CS in a 3% NaCl solution was measured by connecting both electrodes prior to immersing the passive electrode into the solution as shown in Figure 7. As a result, the corrosion of the passive electrode could be delayed or reduced since it was cathodically protected by the corroding electrode. It is shown that the value of I_{gc} obtained on passive CS coupled with corroding CS was very high and reached a stable value at a slower rate in the presence of 3% NaCl. The last column in Table 6 shows the ratio of I_{gc} in the presence of 3% and 0% NaCl in the solution. Compared with the average I_{gc} measured in the saturated $\text{Ca}(\text{OH})_2$ solutions without the addition of NaCl, it was found that the I_{gc} values were considerably higher in passive CS (1.4 times). The increases in SS 2205 and 304LN were also significant (1.9 and 1.5 times) but the I_{gc} values were still lower than those in the passive CS even in the absence of NaCl. However, the galvanic current density on SS 316LN remained at a very low value (with only about a 5% increase) after the addition of 3% NaCl in the solution.

Table 6 - Average I_{gc} ($\mu\text{A}/\text{cm}^2$) for Various Metals Coupled to Corroding CS Measured in Saturated $\text{Ca}(\text{OH})_2$ Solution Containing 0% and 3% NaCl.

Metal	0% NaCl	3% NaCl	Ratio
Passive CS	0.52	0.75	1.4
SS 2205	0.22	0.42	1.9
SS 304LN	0.22	0.33	1.5
SS 316LN	0.22	0.23	1.05

The increase of I_{gc} on SS 2205 in the presence of 3% NaCl is caused by the increase in the cathodic reduction current on its surface. Figure 8(a) shows the cyclic voltammograms of SS 2205 and 316LN measured in a saturated $\text{Ca}(\text{OH})_2$ solution in the absence and presence of 3% NaCl. It was found that both cathodic and anodic current peaks on SS 2205 shifted towards the more positive potential region in the presence of 3% NaCl. This resulted in a substantial increase in the cathodic current near the coupling potential region (about -0.55 V). However this peak shift on SS316LN was not significant [see Figure 8(b)], thus that the cathodic current increase was much smaller near the coupling potential region.

Galvanic Coupling Test in Concrete Specimens

The galvanic behaviour of CS coupled with passive CS or SS in concrete specimens in both the presence and the absence of chlorides, was investigated. The concrete specimens were kept in an environmental chamber with temperatures cycling between 25°C and 45°C (and up to 50°C for a limited period of time) to accelerate the corrosion process. Figures 9 and 10 show the galvanic coupling potential and I_{gc} of active CS coupled with SS in both the presence and the absence of 3.5% chloride ions. In both cases, the active CS was cast in the concrete containing 1.5% chloride ions. The

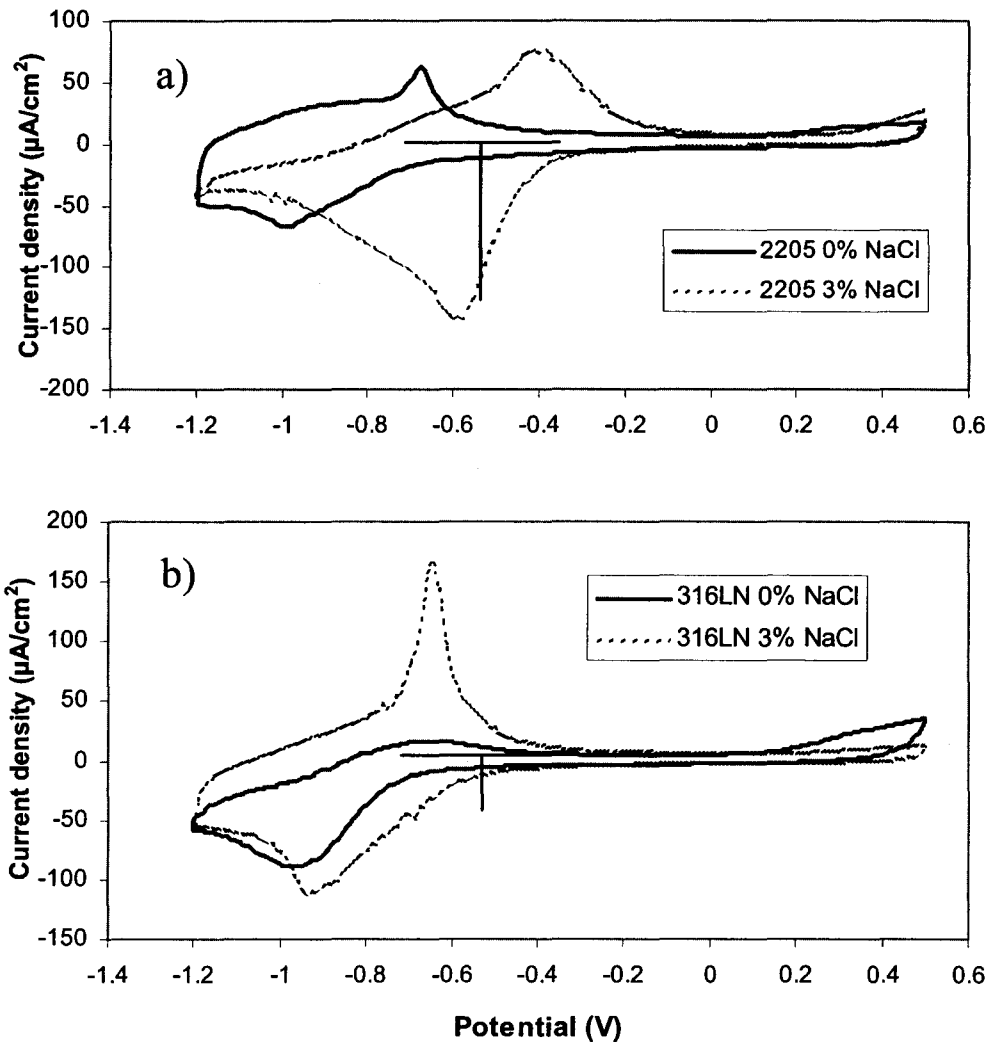


Figure 8 - Cyclic voltammograms of SS measured in a saturated $\text{Ca}(\text{OH})_2$ solution both in the absence and the presence of 3% NaCl: a) SS 2205; b) SS 316LN.

stainless steel specimens were embedded in chloride-free concrete (see Figure 9) or in concrete containing 3.5% chloride ions (see Figure 10). Before coupling the two rebars, the open-circuit potential of the CS was more negative than that of the SS. Since the CS was in the concrete containing 1.5% chloride ions, it was very likely in an active corrosion condition due to the attack of chloride ions. (Corrosion potentials were almost all less than -0.35 V before the coupling.) After the two rebars were connected, the coupling potential was about -0.15 V over 220 days (see Figure 9). During this time, the galvanic coupling current densities were relatively low (about a few nA/cm^2) indicating no considerable galvanic coupling current, even though the CS was in the concrete containing chloride ions. After 220 days, the upper temperature was changed from 45°C to 50°C . The coupling potential shifted to more negative values (about -0.25 V to -0.35

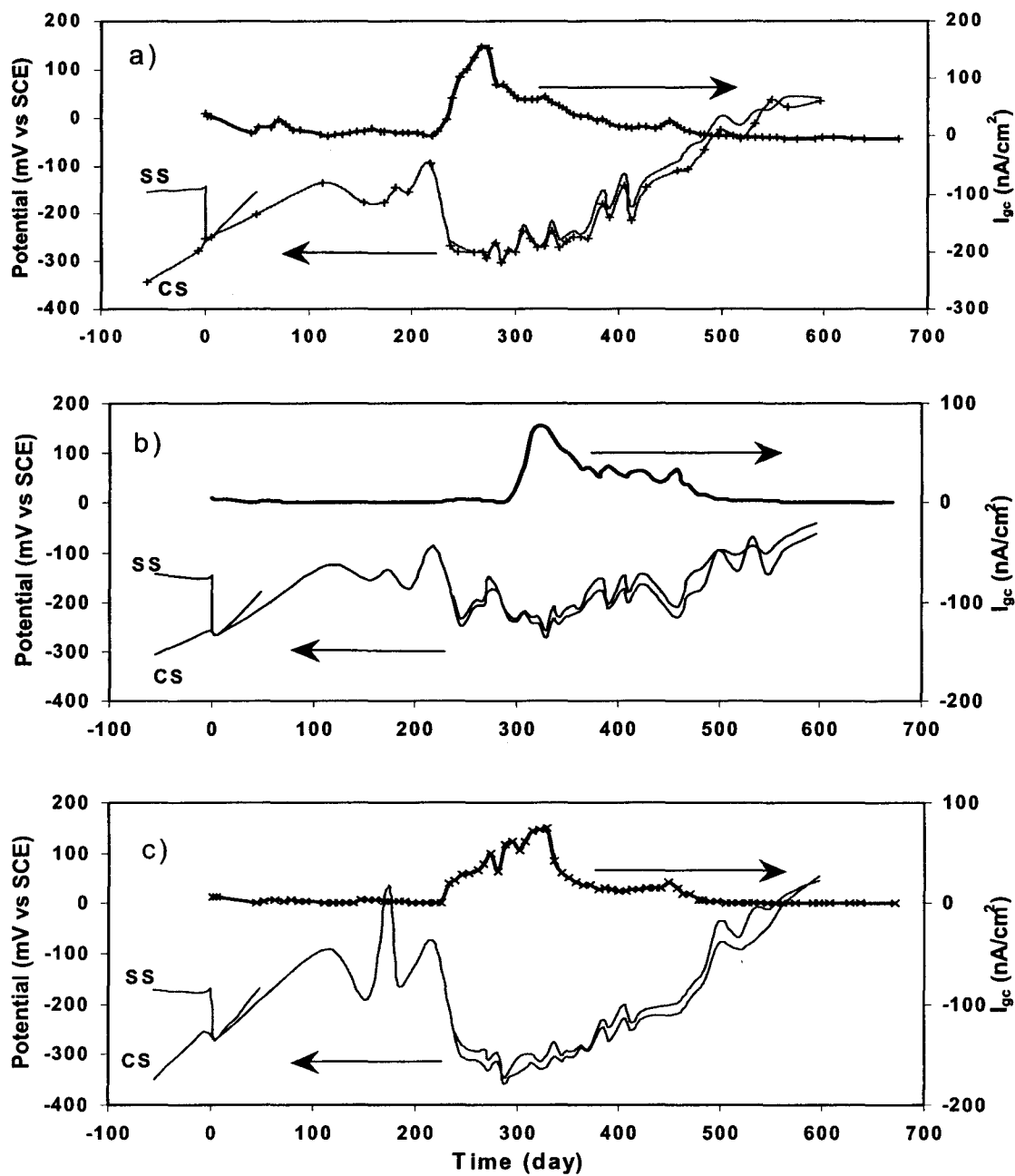


Figure 9 – Galvanic coupling potentials and current densities measured in concrete specimens, for CS in 1.5% Cl⁻ coupled with a SS alloy in a chloride-free environment: (a) SS 2205; (b) SS 304LN; (c) SS 316LN.

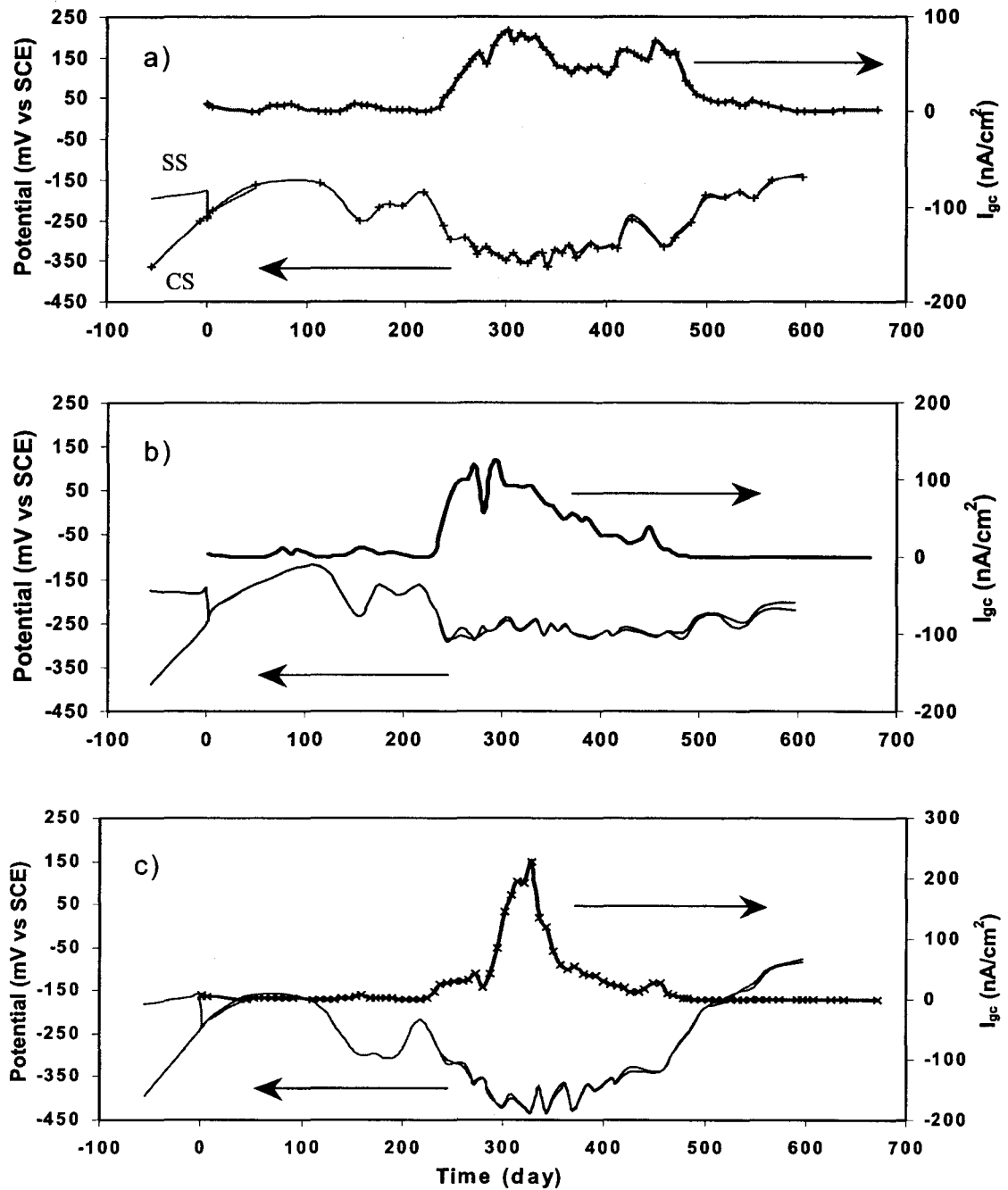


Figure 10 – Galvanic coupling potentials and current densities measured in concrete specimens for CS in 1.5% Cl⁻ coupled with a SS alloy in 3.5% Cl⁻ environment: (a) SS 2205; (b) SS 304LN; c) SS 316LN.

V) and I_{gc} was dramatically increased to around 150 nA/cm² for SS 2205 and 75 nA/cm² for SS 304LN and 316LN, indicating that the corrosion in the active CS had developed significantly. (The increase of I_{gc} was delayed for SS 304LN, probably due to non-uniformities in the temperature, RH of the environmental chamber, or concrete in the specimens. The values of I_{gc} decreased gradually to about 30, 26 and 15 nA/cm² for SS 2205, 304LN and 316LN, respectively, at day 380. This current decrease was probably due to the formation of cracks in the concrete near the corroding CS rebars.

As shown in Figure 10, when SS was subjected to 3.5% chloride ions, the change in coupling potential with time was similar to that shown in Figure 9. After being coupled for about 220 days, the upper temperature in the chamber was changed from 45°C to 50°C, causing the coupling potential to drop to < -0.3 V, and the I_{gc} to increase from 5 nA/cm² to 80, 120 and 200 nA/cm² for SS 2205, 304LN and 316LN, respectively. It is clearly shown that the increase of upper temperature accelerated the development of corrosion in the active CS leading to the increase in I_{gc} . After corrosion product built up around the rebar, concrete cracks appeared in the specimens and the I_{gc} gradually decreased to a very small value due to the increase in the resistance between the steel rebar and concrete. The I_{gc} was slightly higher with SS in concrete containing 3.5% chloride ions than in a chloride-free environment. This may have been caused by two factors: the effect of chlorides on the cathodic reduction reaction on SS or the reduced resistance due to the presence of 3.5% chloride ions in the sides of the specimen in which the stainless steels were embedded.

The galvanic coupling potential and the I_{gc} measured from the active CS coupled with the passive CS are shown in Figure 11. Two carbon steel specimens were embedded in concrete: one in chloride-free concrete and the other in concrete containing 1.5% chloride ions. In the first 220 days, the coupling potential varied around -0.15 V, and the coupling current density remained very low (<10 nA/cm²). After 275 days, the coupling potential dropped to -0.4 V, and the coupling current density increased rapidly to 800 nA/cm² then decreased to about 150 nA/cm² due to concrete cracking near the rebars.

It was clearly shown that the I_{gc} between active and passive carbon steels was much higher than that between active CS and SS, even when the SS was in concrete containing 3.5% chloride ions. This result is in good agreement with that obtained in the saturated Ca(OH)₂ solution in the electrochemical cell. This proves that, with SS reinforcing bars coupled with corroding CS bars, I_{gc} is much lower (less than 200 nA/cm²) than in a coupling between passive and active CS reinforcing bars (about 800 nA/cm²). Therefore, using SS instead of CS reinforcement only in critical areas would not increase the risk of corrosion in the CS reinforcement.

It was also found that, unlike the measurement in the electrochemical cell, the galvanic coupling current in the concrete did not reach its stable value shortly after the coupling. It remained at a very low value over more than 200 days and then increased. This occur because the CS used as an active electrode in the electrochemical cell was

already substantially corroded in the beginning, and its corrosion potential was stable at around -0.55 V to -0.60 V. When this electrode was coupled with passive CS or SS, the observed galvanic coupling behavior was determined by the cathodic reduction reaction on the passive CS or SS. However, the CS used in the concrete specimens was corrosion free before it was cast in the specimens. During the first 200 days, corrosion gradually developed in the CS when exposed to 1.5% chloride ions in concrete. During this time, the measured coupling current was limited by the slow anodic oxidation process on the CS due to its passive film.

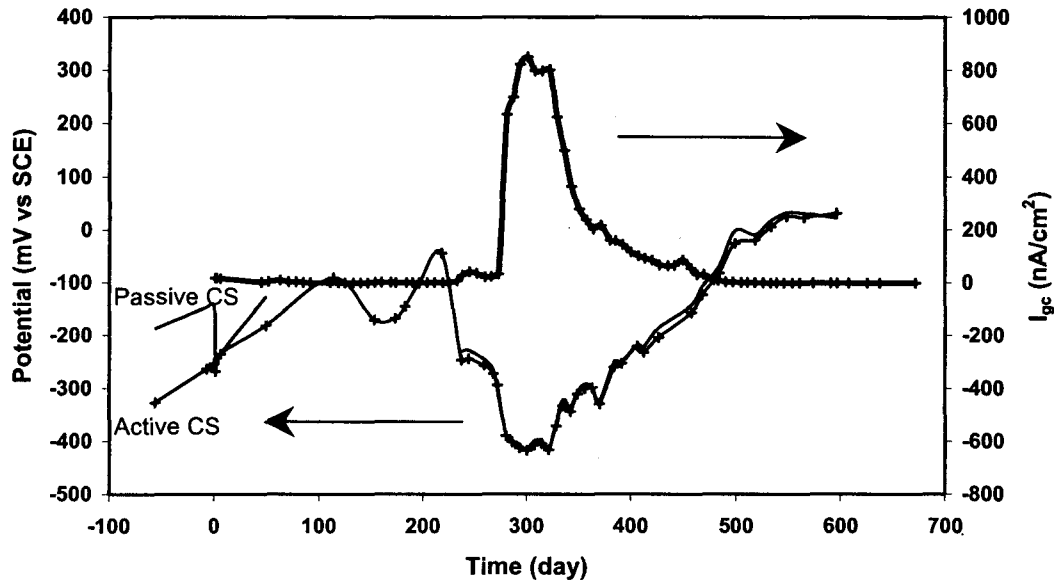


Figure 11 – Galvanic coupling potentials and current densities measured in concrete specimens for CS in 1.5% Cl^- coupled with passive CS in chloride-free environment.

CONCLUSIONS

Based on the above investigation, it can be concluded that use of SS and CS reinforcing bars in the same concrete structure will not increase the corrosion risk on CS even when these bars are in direct (electrical) contact. In fact, the increase in the corrosion rate of CS due to galvanic coupling of SS with corroding CS was less than that of the combination of non-corroded CS with corroding CS. Stainless steel, with its ability to resist chloride-induced corrosion, can be used in areas vulnerable to chloride ingress. Therefore, the judicious use of stainless steel with carbon steel in the high-corrosion-risk areas of a concrete structure can be a cost-effective option for reducing corrosion and greatly extending the service life of concrete structures.

The rate-determining step of the galvanic coupling process is a cathodic reduction reaction on passive CS or SS when these metals are coupled with corroding CS in a saturated $\text{Ca}(\text{OH})_2$ solution. The cathodic reduction current on SS is less than half of that on passive CS, leading to a lower I_{gc} induced by SS.

The increase in corrosion rate on corroding CS is about 2-3% due to the galvanic coupling between corroding CS and passive CS. It is only about 1% due to the coupling between corroding CS and SS. This is based on the experiments carried out on the electrodes having 1:1 apparent surface areas in the saturated $\text{Ca}(\text{OH})_2$ solution. Therefore selective use of SS instead of CS will not be detrimental to the CS in the structure.

In the presence of 3% NaCl, the I_{gc} induced by SS alloys 2205 and 304LN increased due to an increase in the cathodic reduction reaction on these alloys when they were exposed to chloride ions. However, the I_{gc} induced by SS 316LN remained almost unchanged indicating that this type of SS performs better regarding the galvanic coupling effect in concrete that contains chloride.

The galvanic coupling tests carried out in the concrete specimens confirmed the laboratory experimental results. When SS reinforcing bars were coupled with corroding CS bars, the I_{gc} was much smaller than that in a coupling between passive and corroding CS reinforcement.

ACKNOWLEDGMENTS

Grateful acknowledgment is made to The Nickel Institute, Alberta Transportation, The City of Ottawa, The Ministère des Transports du Québec and Valbruna Canada Ltd. for their contributions and support for this research project. Thanks are also due to Bruce Baldock, Glendon Pye, Gordon Chan and Bob Myers of IRC/NRC for their help with the experimental research work.

REFERENCES

1. Bertolini, L., Gastaldi, M., Pastore, T., Pedferri, M.P. and Pedferri, P., "Effects of Galvanic Coupling between Carbon Steel and Stainless Steel Reinforcement in Concrete", International Conference on Corrosion and Rehabilitation of Reinforced Concrete Structures, Orlando, Florida, 1998.
2. Bertolini, L., Gastaldi, M., Pastore, T. and Pedferri, M.P., "Effect of Chemical Composition on Corrosion Behaviour of Stainless Steel in Chloride Contamination and Carbonated Concrete", Properties and Performances,

Proceedings of 3rd European Congress Stainless Steel '99, Vol .3, Chia Laguna, AIM, 1999.

3. Bertolini, L., Pedferri, P., “Laboratory and Field Experience on the Use of Stainless Steel to Improve Durability of Reinforced Concrete”, Corrosion Review, Vol. 20, 2002, 129.
4. Knudsen, A., Jensen, F.M., Klinghoffer, O. and Skovsgaard, T., “Cost-Effective Enhancement of Durability of Concrete Structures by Intelligent use of Stainless Steel Reinforcement”, International Conference on Corrosion and Rehabilitation of Reinforced Concrete Structures, Orlando, Florida, 1998.
5. Knudsen, A., Skovsgaard, T., “Stainless Steel Reinforcement”, Concrete Engineering, Vol. 5, No. 3, 2001, 59.
6. Klinghoffer, O., Frolund, T., Kofoed, B., Knudsen, A., Jensen, F.M. and Skovsgaard, T., “Practical and Economic Aspects of Application of Austenitic Stainless Steel, AISI 316, as Reinforcement in Concrete”, Corrosion of Reinforcement in Concrete: Corrosion Mechanisms and Corrosion Protection, Mietz, J., Polder, R. and Elsener, B., Editors, London, 2000.
7. Cochrane, D.J., “Efficient Use of Stainless Steel Reinforcement for Bridge Structure”, Infrastructure Regeneration and Rehabilitation Improving the Quality of Life Through Better Construction: A Vision for the Next Millennium, Swamy, R.N., Editor, Sheffield Academic Press, Sheffield, 1999.
8. Hope, B., “Some Corrosion Aspects of Stainless Steel Reinforcement in Concrete”, Final Report of MTO Special Project Q900076, ISBN 0-7794-0479-3, MI-181, Feb. 2001.
9. Webster, H.A. “A Discussion on Cell Action as it Refers to Steels in Concrete”, COR-97-7810-N, CORRENG Consulting Service Inc., Downsview, Ontario, 1997.
10. Seibert, P.J., “Galvanic Corrosion Aspects of Stainless and Black Steel Reinforcement in Concrete”, M. Sc Thesis, Queen's University, 1998.
11. Langford, P., Broomfield, J., “Monitoring the Corrosion of Reinforcing Steel”, Construction Repair, Vol. 1, No. 2, Palladian Publications, May 1987, 32-36.